Packing Ovals In Optimized Regular Polygons

Frank J. Kampas [a], János D. Pintér [b], Ignacio Castillo [c,*]

[a] Physicist at Large Consulting LLC, Bryn Mawr, PA, USA
[b] Department of Industrial and Systems Engineering, Lehigh University, Bethlehem, PA, USA
[c] Lazaridis School of Business and Economics, Wilfrid Laurier University, Waterloo, ON, Canada
* Corresponding author. E-mail address: icastillo@wlu.ca

Abstract

We present a model development framework and numerical solution approach to the general problem-class of packing convex objects into optimized convex containers. Specifically, here we discuss the problem of packing ovals (*egg-shaped* objects, defined here as generalized ellipses) into optimized regular polygons in $\mathbb{R}^2$. Our solution strategy is based on the use of embedded Lagrange multipliers, followed by nonlinear (global-local) optimization. The numerical results are attained using randomized starting solutions refined by a single call to a local optimization solver. We obtain credible, tight packings for packing 4 to 10 ovals into regular polygons with 3 to 10 sides in all (224) test problems presented here, and for other similarly difficult packing problems.

Key words: Object Packings · Generalized Ellipses (Ovals, Eggs) · Regular Polygon Containers · Model Development Using Embedded Lagrange Multipliers · Global-Local Nonlinear Optimization · Numerical Test Results.

1 Introduction

The efficient packing, arrangement, or configuration design of objects is required across a vast range of engineering and scientific applications. Industrial engineering (IE) and operations research (OR) applications include facility layout design, cutting stock problems in various contexts (e.g., in the glass, metal, paper, textile, and wood industries), and the packing arrangement of solid objects for storage or transportation. A perfunctory web search for the key words "packing problems" returns more than 150,000 results (as of November 2018). Therefore here we only refer to a relatively small selection of works that present, review and discuss IE/OR packing methods and applications: consult e.g., Dowsland and Dowsland (1992), Lodi *et al.* (2002), Pisinger and Sigurd (2007), Bennell and Oliveira (2008), Castillo *et al.* (2008), Hifi and M'Hallah (2009), Bennell *et al.* (2010), Chernov *et al.* (2010), López and Beasley (2011), Fasano (2014), Fasano and Pintér (2015), Alt (2016), Anjos and Vieira (2017), with many topical references. Let us add that e.g., information theory and error-correcting codes (Conway, 1995; Shannon, 1948), number theory, approximation theory, algebra, and theoretical physics (Cohn, 2010), and the design of experiments (Kleijnen, 2015) are further important application areas.

As stated by Saunders (2017) in his anniversary review article, Thompson's classical work (1917) has stood at the forefront of our understanding of the development of biological

form for the past century. Studies in computational physics, chemistry and biology often search for optimized object configurations. The number of web references related to these topics is in the range of *millions*: here we refer only to a small selection of books by Landau *et al.* (2012), Newman (2012), Kellis (2016), O'Neil (2017).

To give a few concrete examples, object packing studies in the sciences are related, e.g., to the structural analysis of liquids, crystals, and glasses (Bernal, 1959); the flow and compression of granular materials (Edwards, 1994; Jaeger and Nagel, 1992, 1996); the design of high-density ceramic materials and the formation and growth of crystals (Cheng *et al.*, 1999; Rintoul and Torquato, 1996); the thermodynamics of liquid to crystal transition (Alder and Wainwright, 1957; Chaikin, 2000; Pusey, 1991); and the chromosome organization in human cell nuclei (Uhler and Wright, 2013).

The paradigm packing objects *efficiently* leads to interesting model development and (often) hard optimization challenges. A packing configuration can be formally defined as a non-overlapping arrangement of a given collection of objects inside a chosen type(s) of container(s). Packings can be optimized according to some appropriately selected criterion, such as the area or volume of the container or the packing fraction (defined as the fraction of the container area/volume covered by the packed objects). The convexity of the packed objects and/or of the container is often postulated, noting that such problems typically still require non-convex continuous and/or combinatorial optimization approaches.

To start with a seemingly "easy" case, packing identical circles has received considerable attention. Research on packing identical circles frequently aims at proving the optimality of the configurations found, either theoretically or with the help of rigorous computational techniques. Provably optimal configurations, with the exception of certain special cases, are available only for a few tens of circles; best-known results are available for packing up to 2,600 identical circles in a circle and 10,000 identical circles in a square. For further details and references, consult e.g., Szabó *et al.* (2007) or Specht (2018).

The general circle packing problem – considered for a given set of circles with (in principle) arbitrary size – is a substantial generalization of the case with identical circles. In full generality, provably optimal configurations are available only for models with $n \leq 4$ circles. Therefore, studies dealing with such problems introduce and apply efficient generic or tailored global scope numerical solution strategies, but without the ability to prove the optimality of the results obtained. We refer to Castillo *et al.* (2008) and to Hifi and M'Hallah (2009) for reviews of both uniform and arbitrary sized circle packings and their applications. More recently, Pintér *et al.* (2017) present numerical results for general sphere packings in $2, 3, 4, 5$ dimensions with up to 50 spheres.

Compared to circle packings, ellipse packing problems have received relatively little attention in the literature. Finding high quality, globally optimized packings of ellipses with arbitrary size and orientation is a hard computational problem. The key challenge is the modeling and enforcement of the non-overlapping constraints as a function of ellipse center locations and orientations. Galiev and Lisafina (2013) studied of ellipse packing problems assuming identical ellipses, orthogonally oriented inside a rectangular container.

Uhler and Wright (2013) relax these assumptions, and propose a model that minimizes a measure of overlap between ellipses (while overlaps still remain possible). Kallrath (2017) extends the work presented in Kallrath and Rebennack (2014) to pack non-overlapping ellipses of arbitrary size and orientation into optimized rectangular containers: the key modeling idea is to use separating lines to ensure that the ellipses do not overlap with each other. Birgin *et al.* (2017) extend the work presented in Birgin *et al.* (2016) for packing arbitrary ellipses in convex containers: they propose a multi-start strategy combined with starting guesses and a local optimization solver, in order to find good quality packings with up to 1000 ellipsoids. We will refer to our related previous work in Section 3, while extending that work for the more general problem-class studied here. Despite the substantial amount of research effort highlighted above, it is evident that packing relatively "simple" objects such as circles or ellipses into "simple" (circular, rectangular) containers already leads to modeling and optimization challenges.

In this article, we concentrate on model development and numerical solution approaches to the problem of packing more general convex objects using a unified, flexible, accurate, and efficient framework. Our model development relies on representing the objects to be packed by a general convex set-type known as ovals or eggs. (In common English, the term oval is used for any shape which reminds one of an egg.) We will give a formal definition below, noting that – according to our definition – circles and ellipses are special cases of ovals. To further enhance the flexibility of our modeling framework, we consider optimized regular polygons as container sets.

To our best knowledge, there are no previous studies related to the general problem-class studied here. Following this introduction, we define and discuss ovals in Section 2. The optimization model development framework is presented in Section 3. Illustrative numerical results and their analysis are described in Section 4. The conclusions (Section 5) are followed by a fairly extensive list of references.

2 Ovals: General Definition and Some Special Cases

Perhaps surprisingly, there is no unique definition of ovals, egg-shaped curves or bodies. Consult e.g. the topical webpages of Köller (2018) and Yamamoto (2018) for related discussions and a number of alternative definitions.

Citing the "oval" entry of Wikipedia (2018), oval commonly means a shape like an egg or an ellipse. It can be also used to refer to a "stadium" shape defined by two semicircles joined by a rectangle. Sometimes, it can even refer to a rectangle with rounded corners. The general term oval is used also to describe certain non-convex objects such as the lemniscate of Bernoulli, or Cassini ovals.

In this work, we define the contour of an oval curve in $\mathbb{R}^2$ that follows the equation

$$\left(\frac{x}{a}\right)^p + e^{tx}\left(\frac{y}{b}\right)^p = 1. \tag{1}$$

In (1), (x, y) is the location of a point on the oval contour curve in $\mathbb{R}^2$, $a > 0$ and $b > 0$ are the semi-major and semi-minor axes of this curve, $p \geq 2$ is an even integer, and $t \geq 0$ is the distortion factor. An oval can be defined with arbitrary size and orientation parameters, noting that – in the case studied here –the size and distortion factors are limited in order to maintain the oval's convexity. The four images displayed in Figure 1 illustrate the modeling flexibility offered by ovals defined in the form of equation (1), for several settings of the parameters a, b, p, and t. For example, the setting $a = b, p = 2, t = 0$ results in a circle; and the (general) pair of a, b with $p = 2$, $t = 0$ results in an ellipse. Setting $p = 2$ leads to ovals which become more asymmetrical and "pointed" as t increases. Setting $p = 4$ leads to "stadium" like objects, and so on.

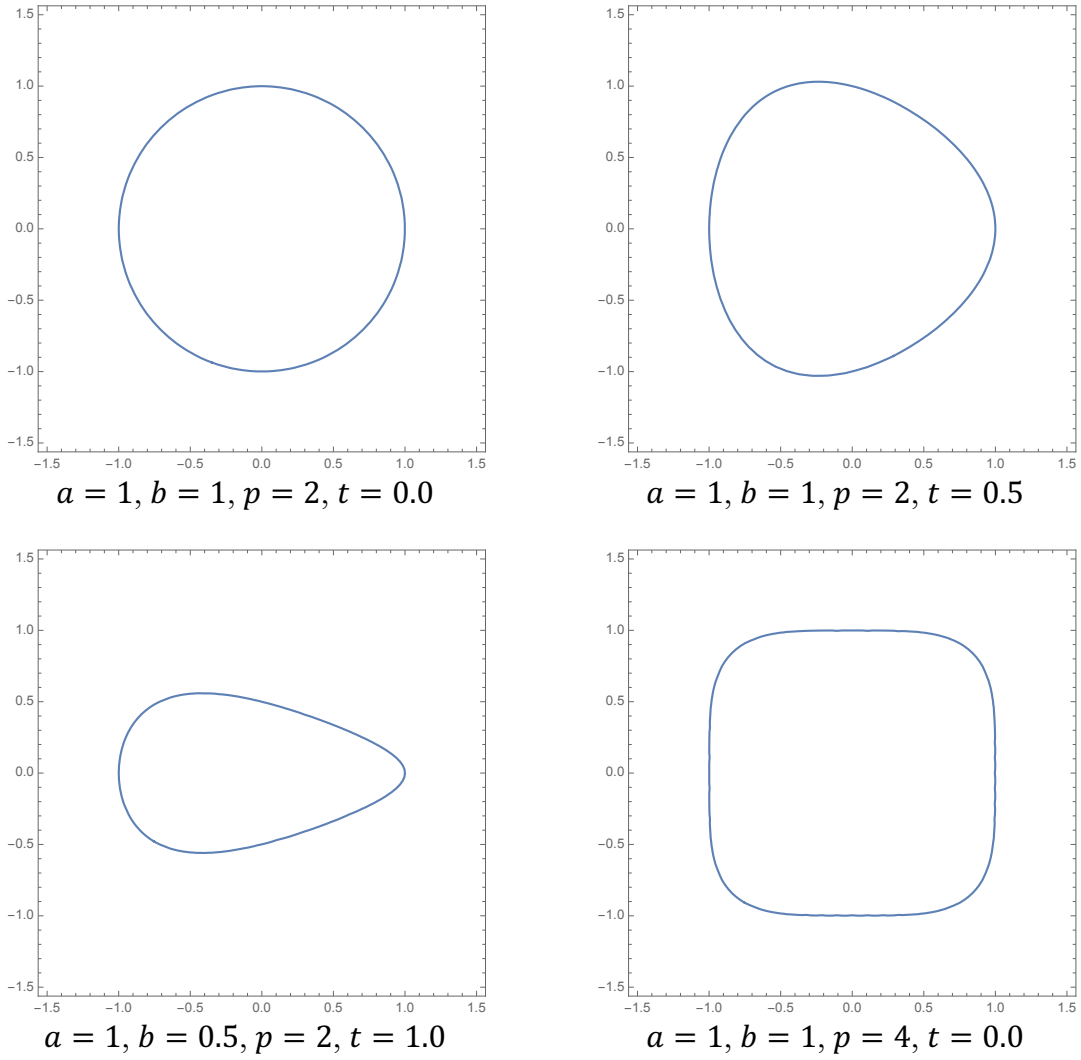

Figure 1. General oval curve examples for several values of a, b, p, and t.

3 Optimization Model Development

Our modeling and solution approach is based on extending the use of embedded Lagrange multipliers to the case of oval objects studied here. Embedded Lagrange multipliers were introduced to pack ellipses inside optimized circular containers in Kampas *et al.* (2017), and to pack ellipses inside optimized regular polygons in Kampas *et al.* (2018).

Here we also use an optimized regular polygon as the container set. The extension from ellipses to ovals is, however, not trivial. Our objective is to minimize the area of the regular polygon that contains a given collection of ovals with arbitrary size and orientation.

The input data to such an optimization problem instance are defined by the number of sides for the container, and the parameters (semi-major, semi-minor axes, exponent and distortion factor) of the ovals to be packed.

The primary decision variables are the polygon's apothem, and the centre position and orientation of each of the packed ovals. (Recall that the apothem of a regular polygon is a line segment from the polygon's center to the midpoint of one of its sides.)

There are two sets of secondary variables. The first set consists of the positions of the distance maximizing lines pointing from each oval boundary to the center of each of the polygon faces. The second set is given by the positions of the points on one of each pair of ovals which minimizes the value of the equation describing the other oval.

The secondary variables are used to define the model constraints. The first set is used to represent the constraints that keep the ovals inside the container. The second set is used to prevent the ovals from overlapping. These constraint sets are generated by embedded Lagrange multiplier conditions. In our optimization strategy, the calculations for finding the polygon's apothem and for preventing oval overlaps proceed simultaneously, rather than being performed to completion at each step towards the minimization of the polygon area.

Denote by m the number of polygon sides, and by d the m-polygon's apothem: the area of this polygon equals $m \cdot d^2 \cdot \tan(\pi/m)$. Since m is an input parameter to the optimization problem instance, minimizing the apothem is equivalent to minimizing the area of the regular m-polygon.

Equation $e(a, b, p, t, xc, yc, \theta; x, y)$ displayed below defines an oval with its given input parameters – semi-major and semi-minor axes a and b, exponent p, and distortion factor t – centered at $\{xc, yc\}$, and rotated counterclockwise by angle θ. Recall that (xc, yc) and θ are the primary decision variables for each oval.

$$e(a,b,p,t,xc,yc,\theta;x,y) = \left(\frac{\cos(\theta)\,(x-xc)+\sin(\theta)\,(y-yc)}{a}\right)^{p} + e^{t\delta}\left(\frac{\cos(\theta)\,(y-yc)-\sin(\theta)\,(x-xc)}{b}\right)^{p} - 1, \quad (2)$$

where $\delta = \cos(\theta)\,(x-xc)+\sin(\theta)\,(y-yc)$.

The value of $e(a,b,p,t,xc,yc,\theta;x,y)$ is negative for all points (x,y) located inside the oval, zero for all points on the oval boundary, and positive for all points outside the oval.

We will assume (postulate) that the optimized polygon container is centered at the origin. Consider now the line $cx\cdot x + cy\cdot y = l$ that embeds one of the sides of the polygon. The slope of this line is $-(cx/cy)$. If (cx,cy) is a unit vector so that $cx^2+cy^2=1$, then the point on the line closest to the origin is $l\cdot(cx,cy)$. The slope of the line to that point is cy/cx: hence, the line from the origin to the closest point on $cx\cdot x + cy\cdot y = l$ is perpendicular to it.

As mentioned above, the first set of constraints is used to keep the ovals inside the container. We find the maximum value of l, denoted by $l^{\max}$, for which the side of the polygon intersects the oval. Our m-polygon derivation follows the first order Karush–Kuhn–Tucker conditions described by Kallrath and Rebennack (2014) for a rectangular container. For the oval to be contained inside the polygon, all sides $cx\cdot x + cy\cdot y$ must be less than or equal to this maximum value. Consider the following equation using λ as the maximizing embedded Lagrange multiplier.

$$cx\cdot x + cy\cdot y = \lambda\cdot e(a,b,p,t,xc,yc,\theta;x,y). \quad (3)$$

Differentiating equation (3) with respect to x, y, and λ, we can numerically obtain the maximum value $l^{\max}$ in the direction (cx,cy).

For example, consider the line defined by $x+y=1$ and the oval defined by $e(1/2,1/3,2,0,0,0,1/2;x,y)$. The maximum value in the direction (cx,cy) is $l^{\max}=0.2444$ with $(x,y)=(0.4000,0.2914)$: this value can be found by numerically solving equation (3). Figure 2 shows the corresponding line-oval configuration.

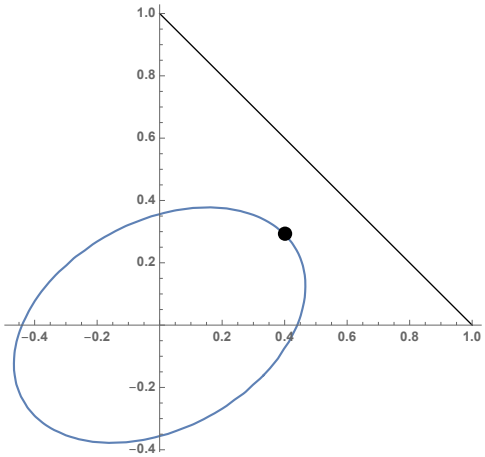

Figure 2. Line-oval configuration in the given example.

Based on the above, the condition of containing a given oval inside the polygon can be described by the relation

$$d \geq l^{\max}(a, b, p, t, xc, yc, \theta; x, y). \tag{4}$$

This constraint will be used in our optimization framework, for all sides of the regular polygon which, of course, share the same apothem distance d. Thus, for a regular polygon with m sides, the points (cx_k, cy_k) that define the unit vectors for each apothem are given by

$$(cx_k, cy_k) = \left(\cos\left(\frac{2 \cdot k \cdot \pi}{m} - \frac{\pi}{2}\right), \sin\left(\frac{2 \cdot k \cdot \pi}{m} - \frac{\pi}{2}\right)\right), k = 1, \ldots, m. \tag{5}$$

Proceeding next towards preventing oval overlaps, it is useful to determine equations for the derivatives of the oval equation with respect to x and y. For a given set of values $(a, b, p, t, xc, yc, \theta)$ we can denote $e(a, b, p, t, xc, yc, \theta; x, y)$ simply as $e(x, y)$: then these derivatives are

$$\frac{de(x,y)}{dx} = -\frac{e^{t\delta} p \varphi^{p-1}}{b} \sin(\theta) + e^{t\delta} t \varphi^p \cos(\theta) + \frac{p \omega^{p-1}}{a} \cos(\theta), \tag{6}$$

$$\frac{de(x,y)}{dy} = \frac{e^{t\delta} p \varphi^{p-1}}{b} \cos(\theta) + e^{t\delta} t \varphi^p \sin(\theta) + \frac{p \omega^{p-1}}{a}, \tag{7}$$

where

$$\varphi = \left(\frac{1}{b}\right)\left((y - yc)\cos(\theta) + (xc - x)\sin(\theta)\right), \tag{8}$$

$$\omega = \left(\frac{1}{a}\right)\left((x - xc)\cos(\theta) + (y - yc)\sin(\theta)\right). \tag{9}$$

All pairs of packed ovals are prevented from overlapping by requiring that the minimum value of the oval equation for oval i for any point on oval j has to be greater than a sufficiently small parameter $\varepsilon \geq 0$. This requirement will be met by using embedded Lagrange multiplier conditions.

The equations shown below determine the point on oval j that maximizes or minimizes the value of the function describing oval i. In the case considered here, λ must be negative to obtain the minimum. During optimization, this requirement with respect to the sign of λ will be enforced by setting its search bounds.

$$\left\{\begin{array}{c} \frac{de(x,y)}{dx}(a_i, b_i, p_i, t_i, xc_i, yc_i, \theta_i; x, y) = \lambda \cdot \frac{de(x,y)}{dx}(a_j, b_j, p_j, t_j, xc_j, yc_j, \theta_j; x, y) \\ \frac{de(x,y)}{dy}(a_i, b_i, p_i, t_i, xc_i, yc_i, \theta_i; x, y) = \lambda \cdot \frac{de(x,y)}{dy}(a_j, b_j, p_j, t_j, xc_j, yc_j, \theta_j; x, y) \\ e(a_j, b_j, p_j, t_j, xc_j, yc_j, \theta_j)(x, y) = 0 \end{array}\right\}. \tag{10}$$

The last equation type introduced corresponds to the requirement that the distance minimizing point lies on oval j. Eliminating λ from the first two equations, we obtain

$$\begin{aligned} \frac{de(x,y)}{dy}(a_i, b_i, p_i, t_i, xc_i, yc_i, \theta_i; x, y) & \\ \cdot \frac{de(x,y)}{dx}\left(a_j, b_j, p_j, t_j, xc_j, yc_j, \theta_j; x, y\right) & \\ = \frac{de(x,y)}{dy}\left(a_j, b_j, p_j, t_j, xc_j, yc_j, \theta_j; x, y\right) & \\ \cdot \frac{de(x,y)}{dx}(a_i, b_i, p_i, t_i, xc_i, yc_i, \theta_i; x, y). & \end{aligned} \tag{11}$$

Let us note that at the point on oval j that minimizes or maximizes the value of the function describing oval i, the slope of oval curve i equals the slope of oval curve j.

For example, consider two ovals defined by $e_i(1,1,2,1/2,0,0,0; x, y)$ and $e_j(1/2,3/4,2,0,0,0,0; x, y)$. The overlap indicator value between the ovals is -0.5924 with $(x, y) = (0.1035, 0.7338)$: this can be found by solving equations (10). Figure 3 shows this (overlapping ovals) configuration.

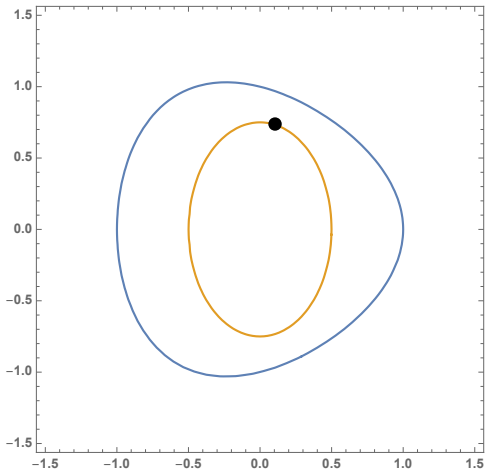

Figure 3. Two overlapping ovals.

To give another example, consider two ovals defined by $e_i(3/4,1,2,1/2,-1/2,0,0;x,y)$ and $e_j(1/3,1/2,2,0,3/4,0,1/2;x,y)$. The overlap indicator value between the ovals is 0.5696 with $(x,y) = (0.3745,0.1004)$: again, this value can be found by solving the set of equations (10) for x and y. Figure 4 shows the resulting (non-overlapping ovals) configuration.

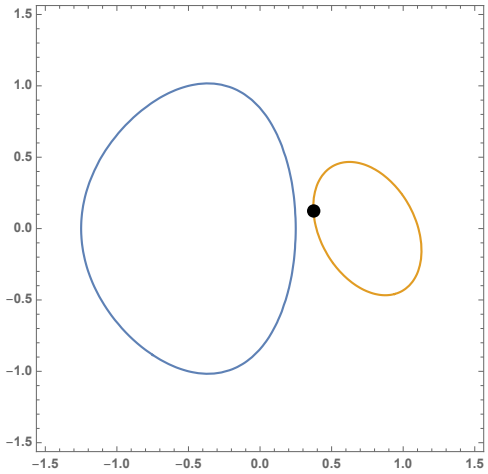

Figure 4. Two non-overlapping ovals.

In our optimization framework, $\lambda_{i,j}$ denote the Lagrange multipliers appearing in the equations to find the point $(x_{j,i}, y_{j,i})$ on oval j that minimizes the value of the equation describing oval i. This calculation is restricted to minimization by requiring that the value of $\lambda_{i,j}$ is negative. Finally, we state constraints to prevent oval i from overlapping with oval j, by requiring that the minimal value of the equation describing oval i at the minimizing point on oval j is at least ε.

Summarizing the model components and development steps discussed above, we present the following model-class for packing n egg-shaped objects (ovals) in an optimized regular m-polygon.

$$\text{minimize} \quad d \tag{12}$$

$$\text{subject to} \quad d \geq l_{i,k}^{\max}(a_i, b_i, p_i, t_i, xc_i, yc_i, \theta_i; cx_k, cy_k) \quad \text{for } i = 1, \dots, n;\ k = 1, \dots, m$$

$$\frac{de(x,y)}{dx}(a_i, b_i, p_i, t_i, xc_i, yc_i, \theta_i; x_{j,i}, y_{j,i}) = \lambda_{j,i} \cdot \frac{de(x,y)}{dx}(a_j, b_j, p_j, t_j, xc_j, yc_j, \theta_j; x_{j,i}, y_{j,i}) \quad \text{for } i = 1, \dots, n-1;\ j = i+1, \dots, n$$

$$\frac{de(x,y)}{dy}(a_i, b_i, p_i, t_i, xc_i, yc_i, \theta_i; x_{j,i}, y_{j,i}) = \lambda_{j,i} \cdot \frac{de(x,y)}{dy}(a_j, b_j, p_j, t_j, xc_j, yc_j, \theta_j; x_{j,i}, y_{j,i}) \quad \text{for } i = 1, \dots, n-1;\ j = i+1, \dots, n$$

$$e(a_j, b_j, p_j, t_j, xc_j, yc_j, \theta_j; x_{j,i}, y_{j,i}) = 0 \quad \text{for } i = 1, \dots, n-1;\ j = i+1, \dots, n$$

$$e(a_i, b_i, p_i, t_i, xc_i, yc_i, \theta_i) \geq \varepsilon \quad \text{for } i = 1, \dots, n-1;\ j = i+1, \dots, n$$

$$lb \leq xc_i \leq ub \quad \text{for } i = 1, \dots, n$$

$$lb \leq yc_i \leq ub \quad \text{for } i = 1, \dots, n$$

$$-\pi \leq \theta_i \leq \pi \quad \text{for } i = 1, \dots, n$$

$$lb \leq x_{j,i} \leq ub \quad \text{for } i = 1, \dots, n-1;\ j = i+1, \dots, n$$

$$lb \leq y_{j,i} \leq ub \quad \text{for } i = 1, \dots, n-1;\ j = i+1, \dots, n$$

$$2 \cdot lb \leq \lambda_{j,i} \leq 0 \quad \text{for } i = 1, \dots, n-1;\ j = i+1, \dots, n$$

In model (12), lb and ub are lower and upper bounds for the oval center positions: these bounds can be chosen appropriately for each oval packing model instance, in order to facilitate the finding of feasible solutions.

We close this section by noting that the embedded Lagrange multiplier conditions used require that the value of the function describing one oval is always greater than (or less than) 0 on all points on the other oval (or line), to ensure that ovals do not overlap with other ovals and that they are located within the polygon container. Analogous conditions are applicable to *any* convex curve described by a function which is always positive for points outside the curve: thus our approach can be applied also to packing rounded polygons.

4 Illustrative Numerical Results

We used a PC running under Windows 7, with an Intel Core i5 processor running at 2.6 GHz, with 16 GBytes of RAM, using *Mathematica* version 11. For the purposes of this study, we have implemented a rather efficient, but simple global-local optimization strategy based on multiple starting points. The numerical experiments are based on using a randomized starting solution used by a single call to the local nonlinear optimization solver Ipopt (2018). While – similarly to all other researchers who address similarly (or even less) difficult general packing problems – we cannot guarantee the theoretical optimality of the configurations found, our computational results consistently lead to visibly good quality packings.

As we stated earlier, to our best knowledge, there are no previously studied model instances available for the general oval packing problem-class considered here. Hence, we created our own test models, by packing ovals of (in principle) arbitrary size and orientation. Table 1 summarizes the oval packing test problem sets considered. Note that setting $p = 2$, $a_i = b_i$, and $t = 0.0$, test case 1 becomes a general circle packing problem for circles with radii $a_i = i^{-1/2}$. With $p = 2$, $a_i > b_i$, and $t = 0.0$, test case 2 becomes a general ellipse packing problem for ellipses with semi-major $a_i = i^{-1/2}$ and semi-minor $b_i = a_i/c$ axes, with eccentricity $c = 2$. Test cases 1-6 and 8 consider ovals with the same distortion factor set ($t = 0.0$, 0.5, or 1.0). Test case 7 considers ovals with different distortion factors $t_i = i/5$.

Tables 2-9 summarize the computational results for a total of 224 oval packing problem instances solved. In these model instances, the number of oval objects is chosen as one of $n = 4, \ldots, 10$; the number of regular polygon container sides is chosen as one of $m = 3,4,5,$ and 10.

Given how difficult these problems are thought to be, we believe that the CPU times (ranging from seconds to several hours, see result tables) are reasonable for our entire range of parameter choices. Note that the result tables also include container area and packing fraction information. Several illustrative packing configurations are displayed in Figure 5. (Similar figures are available, for all examples presented here.)

Considering Tables 2-7, we see that, on average, CPU time increases with the distortion factor t (comparing, e.g., Tables 4-5 and 6-7). On average, CPU time also increases with

the exponent p (comparing Tables 2 and 8). We can also see that, on average, the packing fraction increases with the eccentricity c (comparing, e.g., Tables 2 and 3). In general, there is a positive correlation between the packing fraction and certain functions of the different input parameters. Multiple linear regression analysis, using, for consistency, Tables 2-7 (with $p = 2$ and $t_i = t$ for all instances), indicates that the regression function for the packing fraction can be estimated as $0.8022 + 0.0173 \cdot t + 0.0444 \cdot c - 0.2745 \cdot (1/n) - 0.1905 \cdot (1/m)$. We received *p*-values (i.e., observed significance levels, cf. Black *et al.* (2014)) below 0.0001 for all other input parameters. This finding indicates that we have very strong statistical evidence suggesting that the regression coefficients are different from zero. Figure 6 highlights the quality of our regression equation by depicting actual vs. predicted packing fractions.

To conclude the discussion of numerical results, we note that it is apparent that our global-local optimization strategy could become prohibitively expensive for arbitrarily increasing size collections of ovals, particularly when the ovals are highly distorted and eccentric. Therefore we believe that large-scale problem instances open future research directions towards finding suitable heuristic approaches.

Table 1. Oval packing test cases

Test case	p_i	(a_i, b_i)	t_i
1	2	$\left(i^{-1/2}, a_i\right)$	0.0
2	2	$\left(i^{-1/2}, a_i/2\right)$	0.0
3	2	$\left(i^{-1/2}, a_i\right)$	0.5
4	2	$\left(i^{-1/2}, a_i/2\right)$	0.5
5	2	$\left(i^{-1/2}, a_i\right)$	1.0
6	2	$\left(i^{-1/2}, a_i/2\right)$	1.0
7	2	$\left(i^{-1/2}, a_i\right)$	$i/5$
8	4	$\left(i^{-1/2}, a_i\right)$	0.0

Table 2. Oval packing results for test case 1

Problem number	Number of container sides	Number of ovals	Objective	Area of optimized container	Packing fraction	Time (sec.)
1	3	4	2.6781	9.3169	0.7025	21.7489
2		5	2.8097	10.2554	0.6995	15.5796
3		6	2.8829	10.7962	0.7129	279.985
4		7	2.9296	11.1491	0.7306	71.5815
5		8	3.0304	11.9295	0.7157	589.264
6		9	3.0490	12.0760	0.7360	67.2593
7		10	3.0839	12.3544	0.7448	69.9138
8	4	4	2.1580	9.3137	0.7027	14.0704
9		5	2.1871	9.5668	0.7498	54.0113
10		6	2.2897	10.4850	0.7341	28.3510
11		7	2.3275	10.8340	0.7519	62.3785
12		8	2.3561	11.1021	0.7691	57.7027
13		9	2.3702	11.2353	0.7910	134.182
14		10	2.4040	11.5583	0.7961	110.340
15	5	4	1.9740	9.2647	0.7064	10.7099
16		5	2.0290	9.7887	0.7328	21.9864
17		6	2.0596	10.0855	0.7632	24.0855
18		7	2.1128	10.6139	0.7675	40.0479
19		8	2.1597	11.0903	0.7699	42.5799
20		9	2.1943	11.4487	0.7763	72.4504
21		10	2.2507	12.0438	0.7640	421.234
22	10	4	1.7637	9.1417	0.7159	169.622
23		5	1.8094	9.6219	0.7455	86.3605
24		6	1.8740	10.3211	0.7457	95.7238
25		7	1.9214	10.8499	0.7508	159.780
26		8	1.9391	11.0510	0.7726	330.072
27		9	1.9664	11.3644	0.7820	185.579
28		10	2.0018	11.7771	0.7813	232.406

Table 3. Oval packing results for test case 2

Problem number	Number of container sides	Number of ovals	Objective	Area of optimized container	Packing fraction	Time (sec.)
29	3	4	1.8381	4.3887	0.7457	15.1797
30		5	1.9093	4.7357	0.7574	18.5818
31		6	1.9336	4.8566	0.7924	23.9995
32		7	1.9881	5.1343	0.7933	33.1757
33		8	2.0180	5.2903	0.8070	47.1203
34		9	2.0566	5.4945	0.8088	65.3648
35		10	2.0913	5.6816	0.8098	75.5452
36	4	4	1.4386	4.1391	0.7906	17.1312
37		5	1.5025	4.5148	0.7944	20.1131
38		6	1.5461	4.7809	0.8050	24.5677
39		7	1.5728	4.9476	0.8232	43.7241
40		8	1.6144	5.2123	0.8191	47.2367
41		9	1.6396	5.3765	0.8265	72.3506
42		10	1.6713	5.5863	0.8236	99.1121
43	5	4	1.3064	4.0581	0.8064	15.3050
44		5	1.3535	4.3560	0.8234	22.0519
45		6	1.3909	4.6001	0.8366	29.7306
46		7	1.4281	4.8492	0.8399	40.7732
47		8	1.4614	5.0780	0.8407	52.5977
48		9	1.4904	5.2815	0.8414	72.7178
49		10	1.5118	5.4340	0.8467	85.8090
50	10	4	1.1624	3.9708	0.8241	53.9213
51		5	1.1979	4.2170	0.8505	79.3888
52		6	1.2422	4.5350	0.8486	105.983
53		7	1.2777	4.7978	0.8489	133.923
54		8	1.2974	4.9472	0.8630	177.798
55		9	1.3255	5.1635	0.8606	224.357
56		10	1.3481	5.3408	0.8615	294.655

Table 4. Oval packing results for test case 3

Problem number	Number of container sides	Number of ovals	Objective	Area of optimized container	Packing fraction	Time (sec.)
57	3	4	2.5905	8.7175	0.7548	17.5593
58		5	2.7513	9.8335	0.7331	28.0943
59		6	2.8194	10.3258	0.7490	40.0847
60		7	2.8858	10.8185	0.7564	65.4501
61		8	2.9339	11.1818	0.7670	80.5654
62		9	2.9797	11.5340	0.7738	103.953
63		10	3.0536	12.1128	0.7628	142.606
64	4	4	2.1050	8.8621	0.7425	21.2198
65		5	2.1562	9.2988	0.7753	33.0706
66		6	2.2376	10.0139	0.7723	41.2511
67		7	2.2963	10.5457	0.7759	59.5441
68		8	2.3385	10.9372	0.7841	82.6317
69		9	2.4068	11.5853	0.7704	111.078
70		10	2.4268	11.7785	0.7845	143.685
71	5	4	1.9439	8.9847	0.7324	22.6133
72		5	1.9767	9.2901	0.7760	36.1682
73		6	2.0239	9.7393	0.7941	49.2482
74		7	2.0797	10.2841	0.7957	70.5491
75		8	2.1322	10.8094	0.7934	95.7088
76		9	2.1946	11.4508	0.7794	142.376
77		10	2.2212	11.7306	0.7877	163.732
78	10	4	1.7507	9.0073	0.7305	84.8077
79		5	1.7772	9.2819	0.7767	177.210
80		6	1.8157	9.6893	0.7982	251.449
81		7	1.8767	10.3510	0.7905	246.120
82		8	1.8995	10.6040	0.8088	338.850
83		9	1.9526	11.2051	0.7965	483.244
84		10	1.9793	11.5138	0.8025	632.362

Table 5. Oval packing results for test case 4

Problem number	Number of container sides	Number of ovals	Objective	Area of optimized container	Packing fraction	Time (sec.)
85	3	4	1.8583	4.4860	0.7334	2.7068
86		5	1.9052	4.7153	0.7645	4.1626
87		6	1.9562	4.9708	0.7779	5.3980
88		7	2.0110	5.2534	0.7788	8.0164
89		8	2.0703	5.5678	0.7701	10.4752
90		9	2.0871	5.6585	0.7887	14.5303
91		10	2.1150	5.8110	0.7950	19.1139
92	4	4	1.4501	4.2056	0.7823	3.6087
93		5	1.5141	4.5850	0.7862	5.8385
94		6	1.5525	4.8208	0.8021	7.8616
95		7	1.5782	4.9815	0.8213	9.8326
96		8	1.6043	5.1478	0.8330	14.8706
97		9	1.6495	5.4419	0.8201	19.4581
98		10	1.6936	5.7365	0.8054	23.8477
99	5	4	1.3073	4.0632	0.8097	33.6934
100		5	1.3527	4.3503	0.8286	52.4342
101		6	1.3897	4.5919	0.8421	89.9398
102		7	1.4305	4.8655	0.8409	107.572
103		8	1.4617	5.0797	0.8441	153.185
104		9	1.4905	5.2822	0.8449	919.116
105		10	1.5286	5.5554	0.8316	259.104
106	10	4	1.1646	3.9860	0.8254	128.008
107		5	1.2081	4.2896	0.8403	183.518
108		6	1.2489	4.5842	0.8435	281.481
109		7	1.2769	4.7915	0.8539	954.583
110		8	1.3110	5.0512	0.8489	486.143
111		9	1.3330	5.2218	0.8546	622.763
112		10	1.3559	5.4027	0.8551	1435.69

Table 6. Oval packing results for test case 5

Problem number	Number of container sides	Number of ovals	Objective	Area of optimized container	Packing fraction	Time (sec.)
113	3	4	2.5323	8.3301	0.8026	769.011
114		5	2.6901	9.4009	0.7785	888.957
115		6	2.7724	9.9844	0.7857	1376.57
116		7	2.8754	10.7403	0.7724	4189.08
117		8	2.9253	11.1165	0.7817	3603.15
118		9	3.0084	11.7566	0.7689	5123.83
119		10	3.0549	12.1234	0.7717	6635.19
120	4	4	2.1002	8.8214	0.7579	806.650
121		5	2.1920	9.6100	0.7615	408.624
122		6	2.2683	10.2900	0.7623	2353.17
123		7	2.2841	10.4342	0.7950	1886.77
124		8	2.3317	10.8733	0.7992	5462.55
125		9	2.3803	11.3316	0.7978	5119.08
126		10	2.4475	11.9800	0.7809	7125.15
127	5	4	1.9254	8.8140	0.7586	753.826
128		5	1.9641	9.1721	0.7979	1231.89
129		6	2.0435	9.9285	0.7901	2060.84
130		7	2.1054	10.5396	0.7871	3801.65
131		8	2.1549	11.0405	0.7871	3512.30
132		9	2.1745	11.2429	0.8040	11414.5
133		10	2.2179	11.6956	0.7999	7243.70
134	10	4	1.7674	9.1800	0.7283	144.602
135		5	1.7711	9.2187	0.7938	220.932
136		6	1.8089	9.6169	0.8157	386.938
137		7	1.8542	10.1038	0.8210	2241.72
138		8	1.8674	10.2481	0.8479	1022.57
139		9	1.9245	10.8852	0.8305	844.129
140		10	1.9651	11.3488	0.8243	6043.67

Table 7. Oval packing results for test case 6

Problem number	Number of container sides	Number of ovals	Objective	Area of optimized container	Packing fraction	Time (sec.)
141	3	4	1.8521	4.4561	0.7502	19.9478
142	3	5	1.8946	4.6629	0.7847	61.6953
143	3	6	1.9510	4.9449	0.7932	226.774
144	3	7	2.0160	5.2798	0.7856	484.932
145	3	8	2.0764	5.6007	0.7758	808.216
146	3	9	2.0904	5.6764	0.7963	223.154
147	3	10	2.1299	5.8932	0.7937	1186.28
148	4	4	1.4592	4.2586	0.7850	1021.43
149	4	5	1.4992	4.4952	0.8140	1230.49
150	4	6	1.5558	4.8410	0.8102	1612.22
151	4	7	1.6041	5.1463	0.8060	2545.30
152	4	8	1.6322	5.3282	0.8154	3803.67
153	4	9	1.6629	5.5305	0.8173	5969.19
154	4	10	1.6882	5.6997	0.8207	6740.09
155	5	4	1.3348	4.2363	0.7891	2207.20
156	5	5	1.3775	4.5118	0.8110	3220.68
157	5	6	1.4176	4.7777	0.8210	4472.20
158	5	7	1.4462	4.9729	0.8341	6903.90
159	5	8	1.4881	5.2651	0.8252	6838.76
160	5	9	1.5067	5.3975	0.8374	20883.4
161	5	10	1.5293	5.5610	0.8411	13502.4
162	10	4	1.1859	4.1332	0.8088	192.373
163		5	1.2239	4.4021	0.8312	1399.74
164		6	1.2617	4.6783	0.8384	1937.92
165		7	1.2917	4.9038	0.8458	6500.79
166		8	1.3307	5.2038	0.8349	8730.52
167		9	1.3436	5.3057	0.8519	3542.88
168		10	1.3695	5.5118	0.8486	22030.7

Table 8. Oval packing results for test case 7

Problem number	Number of container sides	Number of ovals	Objective	Area of optimized container	Packing fraction	Time (sec.)
169	3	4	2.6259	8.9576	0.7324	4.4808
170		5	2.8097	10.2554	0.7014	8.1396
171		6	2.8555	10.5919	0.7289	14.4646
172		7	2.9837	11.5647	0.7067	17.0902
173		8	2.9682	11.4449	0.7488	44.3698
174		9	3.0139	11.7999	0.7562	96.7891
175		10	3.0565	12.1355	0.7615	825.447
176	4	4	2.1203	8.9910	0.7297	25.2150
177		5	2.1505	9.2497	0.7776	42.6442
178		6	2.2505	10.1294	0.7622	254.799
179		7	2.3094	10.6664	0.7663	648.593
180		8	2.3073	10.6475	0.8049	491.954
181		9	2.3776	11.3063	0.7892	1249.69
182		10	2.4305	11.8150	0.7821	2829.13
183	5	4	1.9532	9.0707	0.7233	5.1273
184		5	2.0343	9.8391	0.7311	9.3015
185		6	2.0398	9.8929	0.7804	17.5677
186		7	2.1284	10.7706	0.7588	73.7508
187		8	2.1273	10.7596	0.7965	43.6279
188		9	2.1929	11.4336	0.7804	492.502
189		10	2.2566	12.1079	0.7632	185.712
190	10	4	1.7538	9.0400	0.7257	75.2667
191		5	1.7759	9.2686	0.7761	121.193
192		6	1.8182	9.7154	0.7947	196.941
193		7	1.8671	10.2456	0.7977	1287.00
194		8	1.9274	10.9182	0.7849	1409.65
195		9	1.9630	11.3250	0.7879	1761.68
196		10	1.9846	11.5755	0.7983	6089.94

Table 9. Oval packing results for test case 8

Problem number	Number of container sides	Number of ovals	Objective	Area of optimized container	Packing fraction	Time (sec.)
197	3	4	2.8763	10.7470	0.7188	73.1147
198		5	2.9749	11.4967	0.7365	123.432
199		6	3.1845	13.1732	0.6897	151.958
200		7	3.2575	13.7846	0.6975	227.377
201		8	3.4068	15.0769	0.6685	298.352
202		9	3.5440	16.3158	0.6429	358.151
203		10	3.7169	17.9468	0.6052	669.925
204	4	4	2.2294	9.9408	0.7771	67.3030
205		5	2.3802	11.3307	0.7473	125.285
206		6	2.4112	11.6275	0.7813	163.078
207		7	2.4629	12.1321	0.7925	225.838
208		8	2.5937	13.4545	0.7491	311.393
209		9	2.7438	15.0572	0.6967	433.157
210		10	2.9695	17.6357	0.6159	510.207
211	5	4	2.1035	10.5206	0.7343	82.7059
212		5	2.2389	11.9184	0.7104	127.430
213		6	2.2976	12.5509	0.7238	189.892
214		7	2.3291	12.8980	0.7454	299.622
215		8	2.3904	13.5858	0.7418	312.729
216		9	2.5637	15.6268	0.6713	753.623
217		10	2.7022	17.3613	0.6256	757.450
218	10	4	1.9398	11.0588	0.6986	139.701
219		5	2.0385	12.2126	0.6933	210.233
220		6	2.0892	12.8277	0.7082	351.298
221		7	2.1804	13.9716	0.6882	437.045
222		8	2.3291	15.9423	0.6322	538.977
223		9	2.3294	15.9465	0.6578	888.381
224		10	2.4129	17.1113	0.6347	1492.95

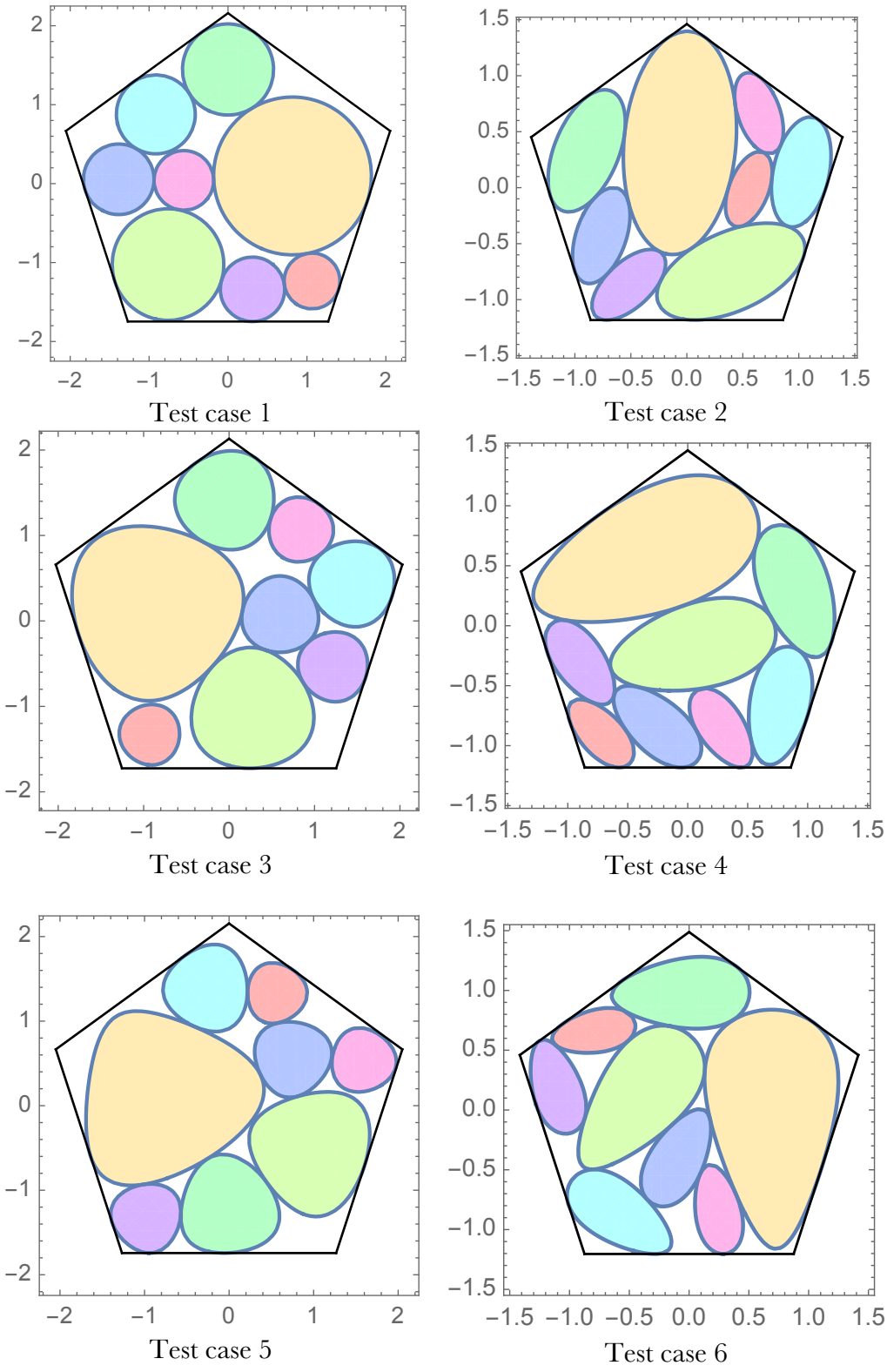

Figure 5. Packing configurations found for $n = 8$ and $m = 5$.

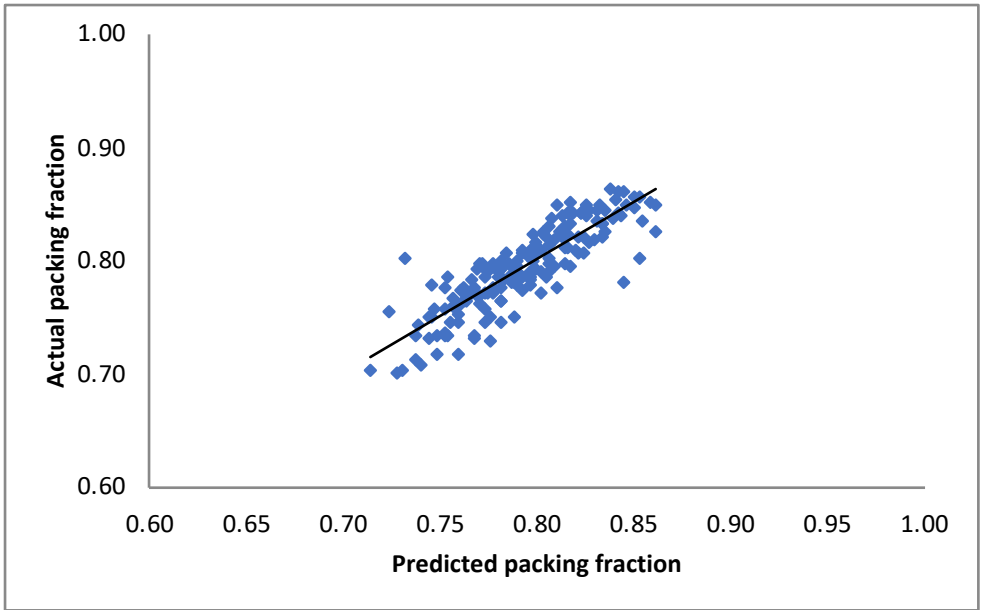

Figure 6. Actual (computed) vs. predicted packing fractions.

5 Conclusions

The efficient packing, arrangement, or configuration design of objects is required across a vast range of engineering and scientific applications. In this work, we present a model development approach to the challenging problem of packing convex planar objects. Specifically, we introduce the general problem-class of packing ovals (defined here as exponentially distorted ellipses) into optimized regular polygons. The numerical solution approach is based on the use of embedded Lagrange multipliers. We produce credible packings for all test problems considered, at the expense of an overall reasonable computational effort. Our embedded Lagrange multipliers based modeling approach is applicable to objects defined by *any* convex curve described by a function which is always positive for points outside the curve. This observation can lead to model development and solution strategies to handle further very general packing problems.

References

Alder, B.J., Wainwright, T.E., 1957. Phase transition for a hard sphere system. *Journal of Chemical Physics* 27, 1208-1209.

Alt, H., 2016. Computational aspects of packing problems. In: *The Algorithmics Column*, *Bulletin of EATCS* 118. European Association for Theoretical Computer Science, www.eatcs.org.

Anjos, M.F. and Vieira, M.V.C., 2017. Mathematical optimization approaches for facility layout problems: The state-of-the-art and future research directions. *European Journal of Operational Research* 261, 1–16.

Bernal, J.D., 1959. Geometrical approach to the structure of liquids. *Nature* 183, 141-147.

Birgin, E.G., Lobato, R.D., Martínez, J.M., 2016. Packing ellipsoids by nonlinear optimization. *Journal of Global Optimization* 65, 709-743.

Birgin, E.G., Lobato, R.D., Martínez, J.M., 2017. A nonlinear programming model with implicit variables for packing ellipsoids. *Journal of Global Optimization* 68, 467-499.

Black, K., Chakrapani, C., Castillo, I., 2014. *Business Statistics for Contemporary Decision Making* (2nd Canadian Edition). Wiley & Sons Canada, Toronto, ON, Canada.

Bennell, J.A. and Oliveira, J.F., 2008. The geometry of nesting problems: A tutorial. *European Journal of Operational Research* 184, 397–415.

Bennell, J.A., Scheithauer, G., Stoyan, Y., and Romanova, T., 2010. Tools of mathematical modeling of arbitrary object packing problems. *Annals of Operations Research* 179, 343–368.

Castillo, I., Kampas, F.J., Pintér, J.D., 2008. Solving circle packing problems by global optimization: Numerical results and industrial applications. *European Journal of Operational Research* 191, 786-802.

Chaikin, P., 2000. Thermodynamics and hydrodynamics of hard spheres: the role of gravity. In: Cates, M.E., Evans, M.R., Eds. *Soft and Fragile Matter: Nonequilibrium Dynamics, Metastability and Flow*, Vol. 53. Institute of Physics Publishing.

Cheng, Z.D., Russell, W.B., Chaikin, P.M., 1999. Controlled growth of hard-sphere colloidal crystals. *Nature* 401, 893-895.

Chernov, N., Stoyan, Yu., Romanova, T., 2010. Mathematical model and efficient algorithms for object packing problem. *Computational Geometry* 43, 535–553.

Cohn, H., 2010. Order and disorder in energy minimization. *Proceedings of the International Congress of Mathematicians*, pp. 2416-2443. Hindustan Book Agency, New Delhi, India.

Conway, J.H., 1995. Sphere packings, lattices, codes, and greed. *Proceedings of the International Congress of Mathematicians*, pp. 45-55. Birkhäuser Verlag, Basel, Switzerland.

Dowsland, K.A. and Dowsland, W.B., 1992. Packing problems. *European Journal of Operational Research* 56, 2-14.

Edwards, S.F., 1994. The role of entropy in the specification of a powder. In: Mehta, A., Ed. *Granular Matter: An Interdisciplinary Approach*. Springer, New York.

Fasano, G. (2014) *Solving Non-standard Packing Problems by Global Optimization and Heuristics*. Springer International Publishing AG, Cham, Switzerland.

Fasano, G. and Pintér, J.D., Eds. (2015) *Optimized Packings with Applications.* Springer International Publishing AG, Cham, Switzerland.

Galiev, S.I., Lisafina, M.S., 2013. Numerical optimization methods for packing equal orthogonally oriented ellipses in a rectangular domain. *Computational Mathematics and Mathematical Physics* 53, 1748-1762.

Hifi, M., M'Hallah, R., 2009. A literature review on circle and sphere packing problems: models and methodologies. *Advances in Operations Research.*
DOI: 10.1155/2009/150624.

Ipopt (2018) https://projects.coin-or.org/Ipopt. The developers of Ipopt are listed at https://projects.coin-or.org/Ipopt/browser/trunk/Ipopt/AUTHORS.

Jaeger, H.M., Nagel, S.R., 1992. Physics of the granular state. *Science* 255, 1523-1531.

Jaeger, H.M., Nagel, S.R., Behringer, R.P., 1996. Granular solids, liquids, and gases. *Reviews of Modern Physics* 68, 1259-1273.

Kallrath, J., 2017. Packing ellipsoids into volume-minimizing rectangular boxes. *Journal of Global Optimization* 67, 151-185.

Kallrath, J., Rebennack, S., 2014. Cutting ellipses from area-minimizing rectangles. *Journal of Global Optimization* 59, 405-437.

Kampas, F.J., Pintér, J.D., Castillo, I., 2017. Optimal packing of general ellipses in a circle. In: Takáč, M. and Terlaky, T., Eds., *Modeling and Optimization: Theory and Applications* (*MOPTA 2016 Proceedings*), pp. 23-38. Springer International Publishing AG, Cham, Switzerland.

Kampas, F.J., Castillo, I., Pintér, J.D., 2018. Optimized ellipse packings in regular polygons using embedded Lagrange multipliers. Research report available for download from *Optimization Online*; www.optimization-online.org/DB_FILE/2016/03/5348.pdf. (Submitted for publication)

Kellis, M., 2016. *Computational Biology: Genomes, Networks, Evolution.* An online textbook for MIT Course 6.047/6.878. Available at
https://ocw.mit.edu/ans7870/6/6.047/f15/MIT6_047F15_Compiled.pdf.

Kleijnen, J.P.C., 2015. *Design and Analysis of Simulation Experiments.* (2nd Edition). Springer US, New York.

Köller, J. (2018) Egg curves and ovals.
http://www.mathematische-basteleien.de/eggcurves.htm.

Landau, R.H., Páez, M.J., and Bordeianu, C.C. 2012. *Computational Physics – Problem Solving with Computers.* Copyright © 2012 by Landau, Páez, and Bordeianu. Copyright © WILEY-VCH Verlag GmbH & Co. KGaA.

Lodi, A., Martello, S., and Vigo, D., 2002. Heuristic algorithms for the three-dimensional bin packing problem. *European Journal of Operational Research* 141, 410–420.

López, C.O. and Beasley, J.E., 2011. A heuristic for the circle packing problem with a variety of containers. *European Journal of Operational Research* 214, 512–525.

Newman, M., 2012. *Computational Physics.* CreateSpace Independent Publishing Platform.

O'Neil, S.T., 2017. *A Primer for Computational Biology*. Oregon State University Press, Corvallis, OR.

Pintér, J.D., Kampas, F.J., Castillo, I., 2017. Globally optimized packings of non-uniform size spheres in R^d: a computational study. *Optimization Letters*, DOI: 10.1007/s11590-017-1194-x.

Pisinger, D. and Sigurd, M., 2007. Using decomposition techniques and constraint programming for solving the two-dimensional bin-packing problem. *INFORMS Journal on Computing* 19 (1), 36–51.

Pusey, P.N., 1991. Colloidal suspensions. In: Hansen, J.P., Levesque, D., Zinnjustin, J., Eds. *Liquids, Freezing and Glass Transition*, Vol. 51 of Les Houches Summer School Session, 763-942. Elsevier Science Publishers, Amsterdam.

Rintoul, M.D., Torquato, S., 1996. Metastability and crystallization in hard-sphere systems. *Physical Review Letters* 77, 4198-4201.

Saunders, T.E. 2017. Imag(in)ing growth and form. *Mechanisms of Development* 145, 13–21.

Shannon, C.E., 1948. A mathematical theory of communication. *The Bell System Technical Journal 27,* 379–423 and 623–656 (July, October 1948).

Specht, E., 2018. http://www.packomania.com/.

Szabó, P.G., Markót, M.Cs, Csendes, T., Specht, E., Casado, L.G., García, I., 2007. *New Approaches to Circle Packing in a Square: With Program Codes.* Springer Science + Business Media, New York.

Thompson, D.W., 1917. *On Growth and Form*. Cambridge University Press.

Uhler, C., Wright, S.J., 2013. Packing ellipsoids with overlap. *SIAM Review* 55, 671-706.

Wäscher, G., Haußner, H., and Schumann, H., 2007. An improved typology of cutting and packing problems. *European Journal of Operational Research* 183, 1109–1130.

Wikipedia (2018) https://en.wikipedia.org/wiki/Oval.

Yamamoto, N. (2018) Equation of egg shaped curve.html.
http://www.geocities.jp/nyjp07/index_egg_E.html